  Bull. Chem. Soc. Jpn., 58, 1484—1489 (1985) [Vol. 58, No. 5

Brillouin Scattering of Supercooled Liquids. I. *Tri-o*-tolyl Phosphate

Shinobu KODA, Hiroyasu NOMURA,* Masayuki NAKAMURA, and Yutaka MIYAHARA
Department of Chemical Engineering, School of Engineering, Nagoya University, Chikusa-ku, Nagoya 464
(Received August 6, 1984)

The sound velocities of *tri-o*-tolyl phosphate in the GHz region were measured by means of the Brillouin scattering method over a wide range of temperatures. In the temperature range from 283 to 313 K, the sound velocity dispersion was observed directly. The relaxation curves of the longitudinal modulus could be analyzed using a B.E.L. model with a parameter of K=0.5. With a rising temperature, a deviation from the B.E.L. model appeared. We considered that the deviation was attributed to the rotational molecular motion of *tri-o*-tolyl phosphate.

Supercooled liquids or glassy materials have abnormally large viscosities compared with those of ordinary liquids. The relaxation times of dynamic shear and bulk viscosities of supercooled liquids are so long that they are within the measurable frequency range. Therefore, the supercooled liquids have been accepted as to be pertinent in clarifying the structure and dynamic properties of liquids.

Earlier investigations of the viscoelastic properties of supercooled liquids have been surveyed by Harrison.[1] Most investigations described were those carried out in the MHz region using ultrasonic and dielectric methods.

Barlow, Lamb and their coworkers[2-6] have extensively studied the viscoelastic properties of many supercooled liquids by means of transverse and longitudinal ultrasonic methods. They showed that the shear modulus of supercooled liquids displays a relaxation phenomena and the distribution of the relaxation times was considerably broader than that predicted from the single Maxwellian relaxation model. It was concluded that the relaxation behavior observed in most supercooled liquids can be described in terms of the generalized B. E. L. (Barlow-Erginsav-Lamb) model.[3]

On the other hand, Litovitz and his coworkers[7-11] have given another description of the relaxation phenomena of supercooled liquids. They indicated that the relaxation behavior of supercooled liquids can be explained by taking account of the distribution of the relaxation times of the cooperative motion of the molecules.[11] Moreover, they measured the relaxation times of the shear and bulk moduli of molten salt, B_2O_3, from 650 to 1000 °C and showed that the shear relaxation process can be represented by a single relaxation time in the temperature range above 800 °C where the shear viscosity is of the Arrhenius type. On the other hand, the shear and bulk relaxation processes exhibit an increasingly broad distribution of relaxation times in the non-Arrhenius region of the lower temperatures.[11] They also found that the master curve of the reduced longitudinal modulus of glycerol in the GHz region is not consitent with the corresponding master curve in the MHz region.[9]

In studying the relaxation phenomena of supercooled liquids, it is necessary to perform experiments over wider temperature and frequency ranges. In order to obtain the longitudinal modulus in the GHz region, the Brillouin scattering method is very useful. Recently, several experimental results regarding supercooled liquids investigated by the Brillouin scattering method have been reported.[12-18] In these works, much attention was given to the Rayleigh dip due to the shear mode of the thermal motion of the molecules in liquids. Scant attention was attracted to the longitudinal mode.

The purpose of this study was to obtain the longitudinal sound velocity in the GHz region for *tri-o*-tolyl phosphate using the Brillouin scattering method as a function of temperature and scattering angle. The sample, *tri-o*-tolyl phosphate, was chosen since its longitudinal and shear moduli in the MHz region have been well investigated by the present authors[19] and Barlow *et al.*[2-6] The longitudinal modulus of *tri-o*-tolyl phosphate in the GHz region is compared with those in the MHz region and a discussion is given regarding the basis of the B. E. L. model. The molecular dynamical investigations of the sample were carried out by means of Raman and depolarized Rayleigh scattering methods.

Experimental

Sample. *Tri-o*-tolyl Phosphate, *tris*(2-methylphenyl) phosphate (practical grade) was obtained from Eastman Organic Chemicals. *Tri-o*-tolyl Phosphate is hereafter abbreviated as TOTP. The sample was purified by fractional distillation under reduced pressure and was checked by Raman spectroscopy.

Brillouin Spectra. The Brillouin spectra were measured using a pressure-scanning Fabry-Perot interferometer. The light source was a He-Ne laser (NEC, GLG 5800) with an output of 50 mw. A detailed description of the apparatus and procedure is found in a previous paper.[20]

In order to obtain the Brillouin spectra over wider temperature ranges, a sample cell (as shown in Fig. 1) was used. This cell was made of Pyrex glass and the diameter of

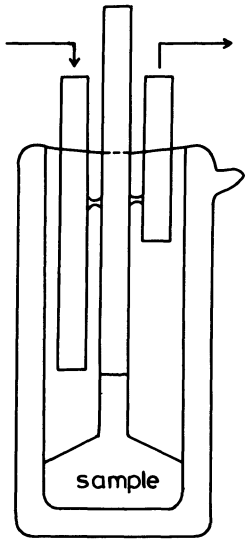

Fig. 1. Brillouin cell. The temperature is regulated by flowing the heated air or cooled air by liquid nitrogen.

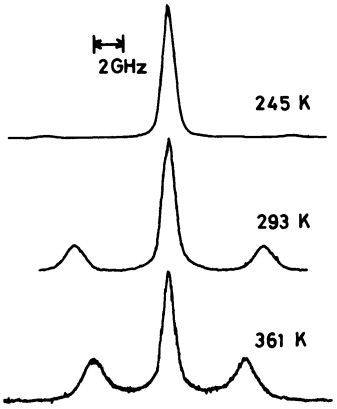

Fig. 2. Representative Brillouin spectra. (θ=90°)

the inner cylinder containing the samle was 5 cm and that of the outer cylinder was 7 cm. The temperature of the sample was regulated by flowing heated and/or cooled air with liquid nitrogen around the inner glass cylinder. The attainable temperature ranges within this cell are from 210 to 350 K with an accuracy of ±1 K. The measured scattering angles were from 20 to 160° for each temerature. The Brillouin spectrum was recorded using an X-Y recorder. At the same time, the spectral intensity and the pressure were punched out on tape as digital data. These data were analyzed to determined the Brillouin frequency shift using a computer.[20] For illustration, the typical Brillouin spectra of TOTP are shown in Fig. 2.

The refractive indexes necessary for the analysis of a sample were measured by means of an Abbe refractometer (Atago) in the temperature range 278 to 337 K.

Raman Spectra. The Raman spectra were measured using a laser Raman Spectrometer JEOL-Ul (Japan Electron Optical Laboratory Co., Ltd.) and an argon ion laser (Coherent Radiation Co., Ltd.), operating at 488 nm (800 mw). The temperature dependence of the Raman spectra was measured with a variable-temperature Raman cell of the Harney-Miller type. The 1047 cm^{-1} band, P-O stretching vibrational mode, of TOTP was measured by using polarizing scattered beam parallel, $I_{\parallel}(\omega)$ and perpendicular, $I_{\perp}(\omega)$ to the electric field vector $\vec{E}$ of the incident light.

Deplorarized Rayleigh Scattering Spectra. The light scattering spectrometer used was consisted of a He-Ne laser (NEC, GLG 5800, 50 mw) and a piezoelectrically driven Fabry Perot interferometer (Burleigh RC 11) with a stabilization system (Burleigh DAS 10, RC 43). The laser beam was irradiated on a sample cell made of quartz. The scattered light at 90° was collimated by a lens through a Glan Thomson prism and the observed spectra were stored in a multichannel analyzer (Anberra Series 30). These spectra could be transfered in a digital form to a microcomputer (Sharp Mz-80c) for further processing. The exeprimental procedures and the correction of instrumental width have been reported elsewhere in details.[21,22] The measuring temperature ranged from 263 to 373 K with an accuracy of±0.5 K.

Results

The sound velocity, V, was calculated from the equation[23]

$$V = \left(\frac{\Delta\omega}{\omega_0}\right)\frac{c}{2n\sin(\theta/2)}, \quad (1)$$

where $\Delta\omega$ is the Brillouin frequency shift, ω_0 the frequency of the incident light, c the velocity of light, n the refractive index of a liquid sample, and θ the scattering angle. The temperature dependence of sound velocities measured at various scattering angles are shown in Fig. 3. It is noted that the constancy of the scattering angle does not always correspond to the constancy of the frequency, because of the temperature dependence of refractive index of a sample. However, as is shown in Fig. 3, at larger scattering angles and lower temperatures, the sound velocity was independent of the scattering angle. This sound velocity can be treated as the sound velocity at the high frequency limit for each temperature. Upon increasing the temperature, the dispersion of sound

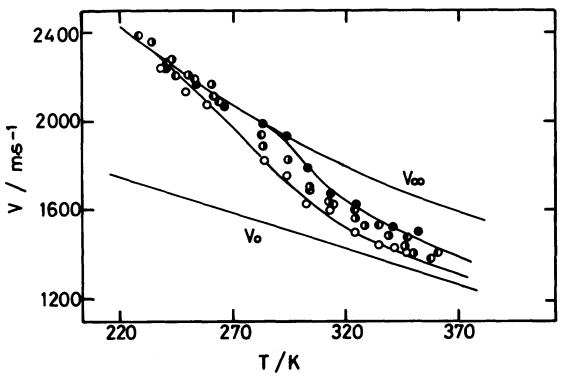

Fig. 3. Temperature dependence of the sound velocity. (●); θ=133°, (◐); θ=90°, (◑); θ=60°, (○); θ=35°.

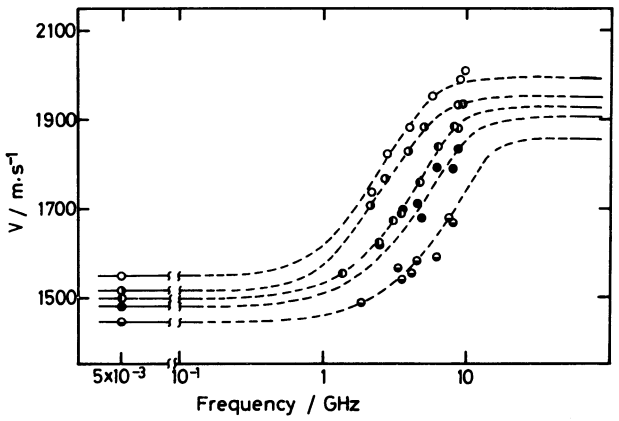

Fig. 4. Frequency dependence of the sound velocity. (○); $T=283$ K, (◑); $T=293$ K, (◐); $T=298$ K, (●); $T=303$ K, (◒); $T=313$ K.

velocity was observed as shown in Fig. 3. On the other hand, Fig. 4 shows the frequency dependence of sound velocity at a constant temperature between 283 and 313 K. The curves clearly show the sound velocity dispersion and the dispersion strength decreases with increasing temperature. In Figs. 3 and 4, the sound velocity at the high frequency limit, V_∞ for each temperature was estimated by extrapolating the V_∞ below 270 K, which were observed directly as shown in Fig. 3. The sound velocity at low frequency limit, V_0, was sometimes measured using by an ultrasonic interferometer working at 4.0 MHz. In wider temperature ranges, the empirical equation proposed by Barlow *et al.*[6] was used.

The Brillouin scattering data also give the Landau-Placzek ratio, $I_R/2I_B$, where I_R and I_B are the intensities of the Rayleigh and Brillouin lines, respectively. However, in this experiment, the accurate intensities of the Rayleigh and Brillouin lines could not be obtained because of the following factors; the diffuse reflection of the cell, a correction of instrumental broadening, the extremely low intensity of Brillouin lines at low temperatures (see Fig. 2) and so on. Therefore, our attention was concentrated upon the Brillouin frequency shift, that is, the sound velocity.

Information regarding the reorientational motion of TOTP can be obtained from an analysis of the Raman line shape[24-26] and/or the depolarized Rayleigh line shape.[27] The half-width refers to the reorientational motion of a molecule, ω_{or}, and can be estimated from the difference between the half-widths of the anisotropic and isotropic Raman lines, $\omega_{anis}(1/2)$ and ω_{isot} (1/2). Details regarding data analysis are presented elsewhere.[28] Figure 5 shows the temperature dependences of $\omega_{isot}(1/2)$ and $\omega_{anis}(1/2)$ after a correction for the broadening effect due to the slit width. As shown in Fig. 5, ω_{or}-

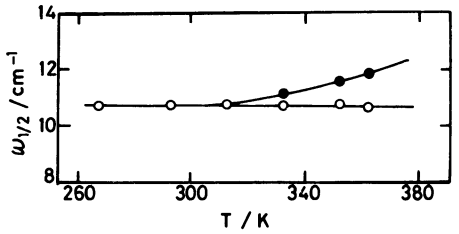

Fig. 5. Temperature dependences of $\omega_{isot}(1/2)$ (○) and $\omega_{anis}(1/2)$ (●).

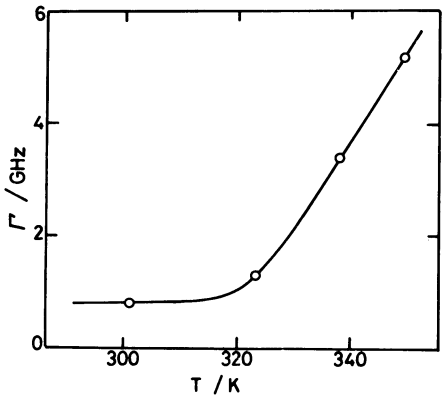

Fig. 6. Temperature dependence of the half-width, Γ, obtained from the depolarized Rayleigh spectrum.

$(=\omega_{anis}(1/2)-\omega_{isot}(1/2))$ was nearly equal to zero at lower temperatures within experimental error, but at a temperature above about 310 K, ω_{or} increased with increasing temperature.

The reorientational correlation times of TOTP can also be obtained from the half-width, Γ, at the half-peak height of the depolarized Rayleigh spectrum.[27] The temperature dependence of Γ after the correction of the instrumental slit width is shown in Fig. 6. In the lower temperature region, the values of Γ do not depend on temperature but at a temperature above 310 K, they increase with increasing temperature.

In the case of a simple molecule, such as a symmetric top, the reorientational correlation time of molecules at a particular molecular axis can be estimated from data of ω_{or} of Raman lines and/or Γ of depolarized Rayleigh lines. However, the molecules such as TOTP are not so simple as to give well defined reorientational correlation times. Therefore, we can not estimate the reorientational correlation time of TOTP from the data of ω_{or} and/or Γ. At least in our opinion, however, ω_{or} and/or Γ can be a measure of the reorientational motion of a molecule in liquids.

Discussion

Generally, there are two mechanisms which give rise to the dispersion of the sound velocity in the GHz region; one is vibrational relaxation due

to an energy transfer from the vibrational mode to the translational motion and the other is the structural relaxation.

The relaxation strength, ε, defined as[29]

$$\varepsilon = \frac{(V_\infty^2 - V_0^2)}{V_0^2}, \tag{2}$$

is shown in Fig. 7 as a function of temperature. The ε, ranging from 220 to 280 K, decreases with increasing temperature. This result indicates that the observed relaxation in this temperature range is not the vibrational relaxation, since the relaxation strength of the vibrational one should increase with temperature.[30] Besides, the value of ε which was estimated theoretically by Planck-Einstein relation was one order of magnitude smaller than those obtained experimentally.[31]

Barlow *et al.* indicated that the relaxation process observed for TOTP in the MHz region can be interpreted as the structural relaxation.[2-6] Figure 8 shows a plot of the longitudinal modulus ($M=1/\rho V^2$) reduced by the shear modulus of the high-frequency limit against the normalized freguency, $\eta\omega/G_\infty$, where η is the viscosity. The values of G_∞ at each temperaure used were those reported previously.[19] The reduced longitudinal moduli result in a master curve within experimental errors. The same quantity

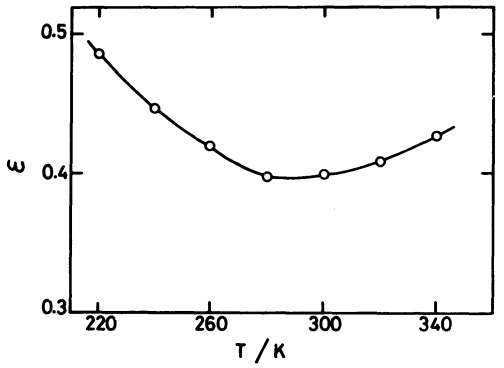

Fig. 7. Temperature dependence of the relaxation strength, ε.

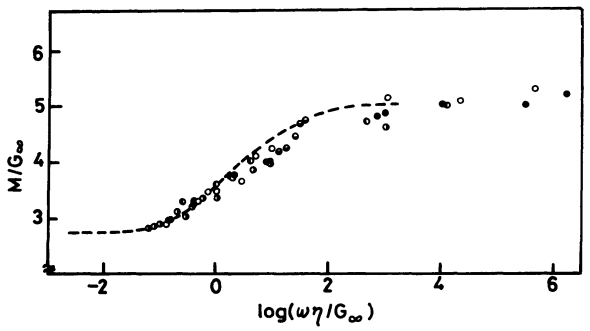

Fig. 8. Values of the reduced longitudinal modulus, M/G_∞, plotted as a function of $\log(\omega\eta/G_\infty)$. The broken line represents the data obtained by Barlow *et al.*[6]

in the MHz region, which was obtained by Barlow *et al.*[6], was compared as in Fig. 8. It seems that the values of M/G_∞ in the GHz region deviate slightly from those in the MHz region.

Various expressions have been used to describe the structural relaxation of supercooled liquids.[1] Such expressions can be classified into two types; one refers to the distribution of the relaxation and the other to the phenomenological parameters. At this stage, it is difficult to determine the distribution function of the relaxation times explicitly and sometimes, a distribution function is assumed. On the other hand, the relaxation behavior of a supercooled liquid in the MHz region is reduced to the normalized curve which is represented by the B. E. L. equation.[3] Moreover, the B. E. L. equation has also been described by a defect-diffusion model at the molecular level.,[32,33] It is worth comparing the applicability of the B. E. L. model to the experimental result in the GHz region.

According to the generalized B. E. L. model,[1,3] the complex compliance $J^*(i\omega)$, is represented by

$$\frac{J^*(i\omega)}{J_\infty^*} = 1 + \frac{G_\infty}{i\eta\omega} + 2K\left(\frac{G_\infty}{i\eta\omega}\right)^{1/2} \tag{3}$$

where J_∞^* is the compliance of the high-frequency limit and K the parameter where $K=0$ corresponds to the single relaxation process of the Mexwellian. Starting from Eq.3, the real parts of the shear, bulk and longitudinal moduli can be estimated. In Figs. 9 and 10, the normalized longitudinal modulus obtained in this experiment is compared with the value estimated from the generalized B. E. L. model. As is seen in Fig. 9, the experimental results are fitted to the generalized B. E. L. model equation, with the value of K being between 0.5 and 1.0. In Fig. 10, the experimental results above $\log(\eta\omega/G_\infty)\geqq 0$ are also reproduced with the generalized B. E. L. equation within experimental errors. The temperature corres-

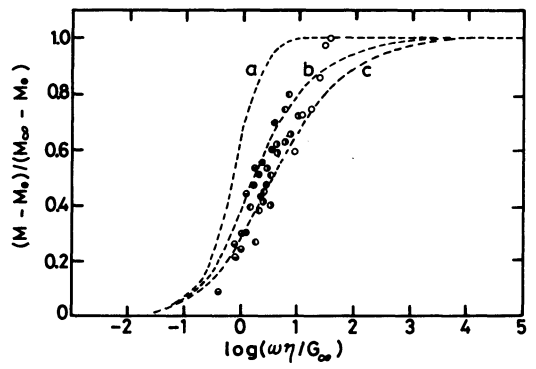

Fig. 9. Values of the normalized longitudinal modulus, $(M-M_0)/(M_\infty-M_0)$ plotted as a function of $\log(\omega\eta/G_\infty)$. The broken lines are calculated for $K=$ 0 (a), 0.5 (b) and 1.0 (c). The symbols are the same in Fig. 4.

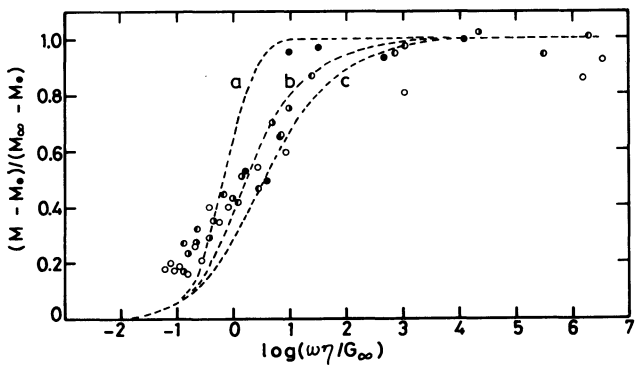

Fig. 10. Values of the normalized longitudinal modulus, $(M-M_0)/(M_\infty-M_0)$ plotted as a function of log $(\omega\eta/G_\infty)$. The broken lines are calculated for K = 0 (a), 0.5 (b) and 1.0 (c). The symbols are the same in Fig. 3.

ponding to $\log(\eta\omega/G_\infty)\simeq 0$ in the GHz region is about 310 K. Therefore,the relaxation of the longitudinal modulus below 310 K is described by the B. E. L. model. Above 310 K, the deviation from the B. E. L. model is appreciable, as can be seen in Fig. 10.

The deviation may be attributed to the following; above 310 K, the dynamic state of TOTP changes and this affects the structural relaxation due to the collective motion of the TOTP molecules. This consideration is supported by the molecular dynamical results of the Raman and depolarized Rayleigh scattering.

The ω_{or} and Γ give information about the molecular motion as described in the previous section. As can be seen in Figs. 6 and 7, the values of ω_{or} and Γ increase with temperature above 310 K. Below that temperature, the value of ω_{or} is nearly equal to zero and that of Γ levels off. These facts indicate that the reorientational motion of TOTP below 310 K is very slow or is almost frozen. Above this temperature, however, reorientational motion will occur. At the same temperature, the temperature dependence of the relaxation strength of sound dispersion of TOTP changed to positive. This asserts that at higher temperatures, the relaxation process may involve the rotational motion of TOTP molecules.

It is a very interesting point how the distribution of relaxation times of the longitudinal modulus relate to the liquid structure and molecular motion. This distribution of relaxation times somewhat depends on the temperature, that is measured frequency ranges (see Fig. 8). At least, we conclude that the deviation from the B. E. L. model at higher temperatures is attributed to the changes of liquid structure of TOTP, especially the changes regarding its dynamical state.

The authors would like to express their appreciation to Dr. T. Kato of Institute of Molecular Science for permission to use the light-scattering spectrometer of depolarized Rayleigh scattering spectra, and also to Mr. T. Watanabe, Glass-technician of Work Shop for Experimentation and Practice, School of Engineering, Nagoya University for making the low temperature cell (see Fig. 1). This work was supported in part by a Grant-in-Aid for Scientific Research from the Ministry of Education, Japan (No. 58540255).

References

1) G. Harrison, "The Dynamic Properties of Supercooled Liquids," Academic Press, London, (1976).
2) A. J. Barlow, J. Lamb, A. J. Matheson, P. R. K. L. Padmini, and J. J. Richter, *Proc. Roy. Soc.*, **A298**, 467 (1967).
3) A. J. Barlow, A. Erginsav, and J. Lamb, *Proc. Roy. Soc.*, **A298**, 481 (1967).
4) A. J. Barlow, A. Erginsav, and J. Lamb, *Proc. Roy. Soc.*, **A301**, 473 (1969).
5) A.J.Barlow and A. Erginsav, *Proc. Roy. Soc.*, **A327**, 175 (1972).
6) A. J. Barlow and R. P. Singth, *J. Chem. Soc., Faraday Trans. 2*, **68**, 1404 (1972).
7) R. Meister, C. J. Marhoeffer, R. Sciamanda, L. Cotter, and T. A. Litovitz, *J. Appl. Phys.*, **31**, 854 (1960).
8) C. J. Montrose, V. A. Solovyev, and T. A. Litovitz, *J. Acoust. Soc. Amer.*, **43**, 117 (1968).
9) D. A. Pinnodw, S. J. Candau, J. T. LaMacchla, and T. A. Litovitz, *J. Acoust. Soc. Amer.*, **43**, 132 (1968).
10) C. J. Montrose and T. A. Litovitz, *J. Acoust. Soc. Amer.*, **47**, 1250 (1970).
11) J. Tauke, T. A. Litovitz, and P. B. Macedo, *J. Amer. Ceram. Soc.*, **51**, 158 (1968)
12) G. D. Enright and B. P. Stoicheff, *J. Chem. Phys.*, **64**, 3658 (1976).
13) Y. Higashigaki and C. H. Wang, *J. Chem. Phys.*, **74**, 3175 (1981).
14) P. J. Chappell, M. P. Allen, R. L. Hallen, and D. Kivelson, *J. Chem. Phys.*, **74**, 5929 (1981).
15) P. Bezot, C. Hess-Bezot, N. Ostrowsky, and B. Ouentrec, *Mol. Phys.*, **39**, 549 (1980)
16) C. H. Wang, *Mol. Phys.*, **41**, 541 (1980).
17) G. Fytas, C. H. Wang, D. Lilge, and Th. Dorfmuller, *J. Chem. Phys.*, **75**, 4247 (1981).
18) C. H. Wang and Quan-L. Liu, *J. Chem. Phys.*, **78**, 4263 (1983).
19) H. Nomura, H. Shimizu, M. Kato, and Y. Miyahara, *Rept. Prog. Polym. Phys. Jpn*, **21**, 109 (1978).
20) H. Nomura, H. Shimizu, Y. Tanaka, S. Koda, T. Okunishi, S. Kato, and Y. Miyahara, *Bull. Chem. Soc. Jpn.*, **55**, 3899 (1982).
21) T. Kato, M. Yudasaka, and T. Fujiyama, *Bull. Chem. Soc. Jpn.*, **54**, 1632 (1981).
22) N. Itoh and T. Kato, *J. Phys. Chem.*, **88**, 801 (1984).
23) I. L. Fabelinskii, "Molecular Scattering of Light," Plenum Press, New York, (1968) p 86.
24) W. G. Rothschild, "Dynamics of Molecular Liquids," John Wiley & Sons, New York, (1984).
25) F. J. Baltoli and T. A. Litovitz, *J. Chem. Phys.*, **56**, 404, 413 (1972).

26) J. E. Griffiths, M. Clerc, and P. M. Rentzepis, *J. Chem. Phys.*, **60**, 3824 (1974).
27) B. J. Berne and R. Pecora, "Dynamic Light Scattering," John Wiley & Sons, New York, (1976).
28) S. Koda, H. Nomura, and Y. Miyahara, *Bull. Chem. Soc. Jpn.*, **52**, 1828 (1981).
29) K. F. Herzfeld and T.A.Litovitz, "Absorption and Dispersion of Ultrasonic Waves," Academic Press, New Yowk, (1959).
30) For example, K. Takagi, and K.Negishi, *J. J. Appl. Phys.*, **16**, 1319 (1977).
31) In calculation, the vibrational frequencies of TOTP are 167, 180, 270, 452, 525, 560, 592, 608, 702, 726, 769, 800, 992, 1048, 1157, 1243, 1383, and 1589 cm^{-1}, whose values are obtained from the Raman spectrum of TOTP. The vibrational frequencies of the infrared active modes are not taken into account, but the corrected value may not be beyond twice.
32) S. Glarum, *J. Chem. Phys.*, **33**, 639 (1960).
33) M. C. Phillips, A. J.Barlow, and J. Lamb, *Proc. Roy. Soc.*, **A329**, 193 (1972).